Thermochimica Acta 475 (2008) 33–38

Contents lists available at ScienceDirect

Thermochimica Acta

journal homepage: www.elsevier.com/locate/tca

Heat capacity, enthalpy and entropy of strontium niobate $Sr_2Nb_2O_7$ and calcium niobate $Ca_2Nb_2O_7$

J. Leitner[a,*], M. Hampl[a], K. Růžička[b], M. Straka[b], D. Sedmidubský[c], P. Svoboda[d]

[a] Department of Solid State Engineering, Institute of Chemical Technology Prague, Technická 5, 166 28 Prague 6, Czech Republic
[b] Department of Physical Chemistry, Institute of Chemical Technology Prague, Technická 5, 166 28 Prague 6, Czech Republic
[c] Department of Inorganic Chemistry, Institute of Chemical Technology Prague, Technická 5, 166 28 Prague 6, Czech Republic
[d] Department of Condensed Matter Physics, Faculty of Mathematics and Physics, Charles University, Ke Karlovu 5, 120 00 Prague 2, Czech Republic

ARTICLE INFO

Article history:
Received 22 January 2008
Received in revised form 6 June 2008
Accepted 20 June 2008
Available online 5 July 2008

Keywords:
Enthalpy increments
Heat capacity
Entropy
Calorimetry
Strontium niobate
Calcium niobate

ABSTRACT

The heat capacity and the enthalpy increments of strontium niobate $Sr_2Nb_2O_7$ and calcium niobate $Ca_2Nb_2O_7$ were measured by the relaxation time method (2–300 K), DSC (260–360 K) and drop calorimetry (720–1370 K). Temperature dependencies of the molar heat capacity in the form $C_{pm} = 248.0 + 0.04350T - 3.948 \times 10^6/T^2\ J\,K^{-1}\,mol^{-1}$ for $Sr_2Nb_2O_7$ and $C_{pm} = 257.2 + 0.03621T - 4.434 \times 10^6/T^2\ J\,K^{-1}\,mol^{-1}$ for $Ca_2Nb_2O_7$ were derived by the least-square method from the experimental data. The molar entropies at 298.15 K, $S^\circ_m(298.15\,K) = 238.5 \pm 1.3\ J\,K^{-1}\,mol^{-1}$ for $Sr_2Nb_2O_7$ and $S^\circ_m(298.15\,K) = 212.4 \pm 1.2\ J\,K^{-1}\,mol^{-1}$ for $Ca_2Nb_2O_7$, were evaluated from the low-temperature heat capacity measurements.

1. Introduction

Strontium niobate $Sr_2Nb_2O_7$ (S2N) is a ferroelectric material with high Curie temperature $T_C = 1615$ K and promising piezoelectric and electro-optical properties. It is also a component of practically important solid solutions $Sr_2(Nb,Ta)_2O_7$ and $(Sr,Ba)_2Nb_2O_7$ for ferroelectric memories based on field effect transistors and capacitors. Single crystals of calcium niobate $Ca_2Nb_2O_7$ (C2N) have been studied as non-linear optical materials and hosts for rare-earth ions. To assess the thermodynamic stability and reactivity of strontium and calcium niobates under various conditions during their preparation, processing and operation, a complete set of consistent thermodynamic data including heat capacity, entropy and enthalpy or Gibbs energy of formation is necessary.

Heat capacity measurements on single crystal S2N have been reported by Akishige et al. [1]. The measurements were performed by the relaxation time method (2–250 K) and adiabatic calorimetry (200–600 K). They observed a λ-type anomaly on the heat capacity curve at $T_{INC} = 495$ K with an incommensurate phase transition of the orthorhombic phase. The corresponding enthalpy and entropy changes are $\Delta H = 291\ J\,mol^{-1}$ and $\Delta S = 0.587\ J\,K^{-1}\,mol^{-1}$. Heat capacity of a monocrystalline S2N has been measured by Shabbir et al. [2,3] by the MDSC method. They found $T_{INC} = 487 \pm 2$ K, $\Delta H = 147 \pm 14\ J\,mol^{-1}$ and $\Delta S = 0.71 \pm 0.10\ J\,K^{-1}\,mol^{-1}$. Curiously, their values of C_{pm} around T_{INC} are half of the results reported in ref. [1].

A thermodynamic assessment of the $SrO–Nb_2O_5$ system has been performed by Yang et al. [4] and the thermodynamic functions of S2N were evaluated. They used Calphad approach for the assessment and phase equilibrium data according to ref. [5]. The enthalpy and entropy of formation of S2N from the constituent binary oxides ($2SrO + Nb_2O_5$) were $\Delta_{f,ox}H = -367.43\ kJ\,mol^{-1}$ and $\Delta_{f,ox}S = -39.93\ J\,K^{-1}\,mol^{-1}$.

The Gibbs energy of formation of C2N from the component oxides has been determined in the temperature range 1225–1287 K with a CaF_2 solid electrolyte galvanic cell [6], $\Delta_{f,ox}G = -178.4 \pm 1.5\ kJ\,mol^{-1}$. The heat capacity and the enthalpy increments of C2N have not been measured.

In a systematic study of thermochemical properties of complex oxides in the $Bi_2O_3–CaO–SrO–Nb_2O_5–Ta_2O_5$ system, we have recently measured heat capacities and enthalpy increments of $Bi_2Ca_2O_5$, Bi_2CaO_4, $Bi_6Ca_4O_{13}$, $Bi_{14}Ca_5O_{26}$ [7], $BiNbO_4$, $BiTaO_4$ [8], $BiNb_5O_{14}$ [9], $SrBi_2Nb_2O_9$, $SrBi_2Ta_2O_9$ [10] and $SrNb_2O_6$ [11]. The aim of this work is the measurement of heat capacity and enthalpy increments of strontium niobate $Sr_2Nb_2O_7$ and calcium niobate $Ca_2Nb_2O_7$ in a broad temperature range, and evaluation of the

* Corresponding author. Fax: +420 220 444 330.
E-mail address: Jindrich.Leitner@vscht.cz (J. Leitner).

0040-6031/$ – see front matter © 2008 Elsevier B.V. All rights reserved.
doi:10.1016/j.tca.2008.06.010

standard molar entropy of these ternary oxides at 298.15 K, as well as the temperature dependence of C_{pm} above room temperature.

2. Experimental

The samples were prepared by conventional solid-state reactions from high purity precursors $SrCO_3$ (99.9%, Aldrich), $CaCO_3$ (99.9%, Aldrich) and Nb_2O_5 (99.85%, Alfa Aesar). The stoichiometric amounts of $SrCO_3$ and Nb_2O_5 were ground in agate mortar and calcined at 1273 K in platinum crucible in air atmosphere for 48 h. After regrinding, the mixture was fired at 1673 K in air for 100 h. In the case of $CaCO_3$ and Nb_2O_5 mixture, calcination was performed at 1073 K (48 h) and the final heat treatment at 1273 K (142 h).

X-ray powder diffraction data were collected at room temperature with an X'Pert PRO (PANalytical, The Netherlands) θ–θ powder diffractometer with parafocusing Bragg–Brentano geometry using Cu Kα radiation (λ = 1.5418 Å, U = 40 kV, I = 30 mA). Data were scanned over the angular range 5–60° (2θ) with an increment of 0.02° (2θ) and a counting time of 0.3 s per step. Data evaluation was performed by means of the HighScore Plus software package.

The PPMS equipment 14 T-type (Quantum Design, USA) was used for the heat capacity measurements in the low-temperature region. The measurements were performed by the relaxation method [12] with fully automatic procedure under high vacuum (pressure ~10^{-2} Pa) to avoid heat loss through the exchange gas. The samples were compressed powder plates of about 15 mg. The densities of the pressed samples were about 65% of the theoretical ones. The samples were mounted to the calorimeter platform with cryogenic grease Apiezon N (supplied by Quantum Design). The procedure was as follows: First, a blank sample holder with the Apiezon only was measured in the temperature range 2–300 K to obtain background data, then the sample plate was attached to the calorimeter platform and the measurement was repeated in the same temperature range with the same temperature steps. The sample heat capacity was then obtained as a difference between the two data sets. This procedure was applied, because the heat capacity of Apiezon is not negligible in comparison with the heat capacity of the sample (~8% at room temperature) and exhibits a sol–gel transition below room temperature [13]. The manufacturer claims the precision of this measurement better then 2% [14]; the control measurement of the copper sample (99.999% purity) confirmed this precision at least below 250 K. However, the precision of the measurement strongly depends on the thermal coupling between the sample and the calorimeter platform. Due to unavoidable porosity of the sample plate this coupling rapidly worsens at temperatures above 270 K as Apiezon diffuses into the porous sample and the uncertainty tends to be larger.

A Micro DSC III calorimeter (Setaram, France) in the incremental temperature scanning mode with a number of 5–10 K steps (heating rate 0.2 K min^{-1}) followed by isothermal delays of 9000 s was used for the heat capacity determination in the temperature range of 260–350 K. Synthetic sapphire, NIST Standard reference material no. 720, was used as the reference material. The typical sample mass was ~0.4 g. The uncertainty of heat capacity measurements is estimated to be better than ±1%.

Enthalpy increment determinations were carried out by drop method with a high-temperature calorimeter, Multi HTC 96 (Setaram, France). All measurements were performed in air by alternating dropping of the reference material (small pieces of synthetic sapphire, NIST Standard reference material no. 720) and of the sample (S2N or C2N pellets, 5 mm in diameter, thickness of 1–2 mm) being initially held at room temperature (T_0), through a lock into the working cell of the preheated calorimeter. Endothermic effects are detected and the relevant peak area is proportional to the heat content of the dropped specimen. The measurements were performed at temperatures 723–1372 K on samples of 100–150 mg. The delays between two subsequent drops were 40–50 min. To check the accuracy of measurement, the heat content of platinum was measured first and compared with published values [15–17]. Estimated overall accuracy of the drop measurements is ±3%.

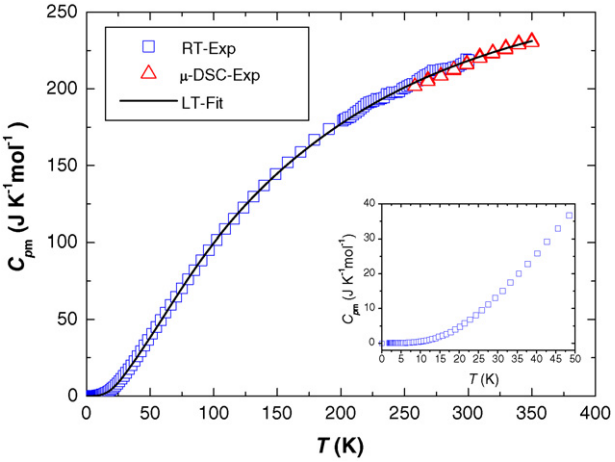

Fig. 1. Low-temperature heat capacity of $Sr_2Nb_2O_7$.

3. Results and discussion

The XRD analysis revealed that the prepared samples were without any observable diffraction lines from unreacted precursors or other phases. The S2N sample was orthorhombic (space group $Cmc2_1$). The following lattice parameters were evaluated by Rietveld refinement: a = 0.395444 ± 0.000017 nm, b = 2.677354 ± 0.000130 nm, and c = 0.570041 ± 0.000026 nm. They are in excellent agreement with the values published recently [18]: a = 0.39544(7) nm, b = 2.6767(6) nm, and c = 0.56961(8) nm. The C2N sample was monoclinic (space group $P2_1$) with refined parameters: a = 0.768528 ± 0.000012 nm, b = 1.335868 ± 0.000040 nm, c = 0.549586 ± 0.000010 nm, and γ = 98.2864 ± 0.0098°, compared with the literature values [19]: a = 0.7697(2) nm, b = 1.3385(6) nm, c = 0.5502(1) nm, and γ = 98.34(6)°. The corresponding densities derived from the above given lattice parameters are 5.21 g cm^{-1} for S2N and 4.50 g cm^{-1} for C2N.

The measured data for S2N involve 124 C_{pm} values from relaxation time, 74 points from DSC and 25 values of the enthalpy increments from the drop measurements. For C2N, 122 C_{pm} values from relaxation time, 28 points from DSC and 14 values of the enthalpy increments from the drop measurement were obtained. C_{pm} data are plotted in Figs. 1 and 2 and summarized in Supplementary Tables 1–4, enthalpy increment data are listed in Tables 1 and 2.

The fit of the low-temperature heat capacity data consists of two steps. Assuming the validity of the phenomenological formula $C_{pm,el} = \beta T^3 + \gamma_{el} T$, where β is proportional to the Debye temperature and γ_{el} is the Sommerfeld term, we plot the C/T vs. T^2 dependence for T < 7 K to estimate the γ_{el} value. As expected, the electronic specific heat is negligible in both samples, C2N and S2N, yielding the respective γ_{el} values 3×10^{-5} and 3.6×10^{-4} J mol^{-1} K^{-2}, which contribute to the heat capacity at the room temperature by 9×10^{-3} and 0.11 J mol^{-1} K^{-1}, respectively, well within the experimental error. It should be noted that the 10 times higher value of γ_{el} in S2N might be due to impurities or some kind of disorder, which either bring about a population of itinerant charge carriers or give rise to a series of Schottky effects. Simultaneously, the C/T vs. T^2 plot provides an estimation of the

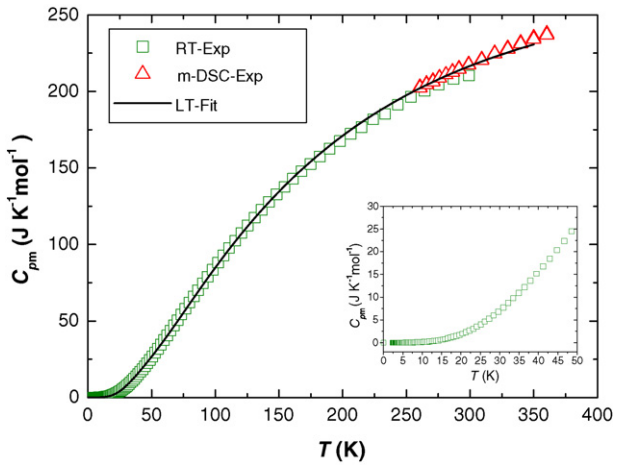

Fig. 2. Low-temperature heat capacity of $Ca_2Nb_2O_7$.

Table 1
Enthalpy increments of strontium niobate $Sr_2Nb_2O_7$

T (K)	$H_m(T) - H_m(298.15)$ (kJ mol^{-1}), experimental	$H_m(T) - H_m(298.15)$ (kJ mol^{-1}), integration of Eq. (4)	δ (%)[a]
773	118.8	120.7	1.6
773	121.7	120.7	−0.8
824	138.4	134.8	−2.6
824	132.0	134.8	2.1
873	151.9	148.5	−2.2
873	147.1	148.5	1.0
924	164.4	162.9	−0.9
924	168.0	162.9	−3.0
924	163.4	162.9	−0.3
973	173.2	176.9	2.1
1024	189.2	191.5	1.3
1024	190.7	191.5	0.4
1024	194.5	191.5	−1.5
1073	213.7	205.7	−3.7
1073	208.0	205.7	−1.1
1124	228.0	220.6	−3.2
1124	214.4	220.6	2.9
1173	235.4	235.1	−0.1
1173	231.5	235.1	1.6
1223	257.3	250.0	−2.8
1224	243.0	250.3	3.0
1224	246.1	250.3	1.7
1273	258.1	265.0	2.7
1273	257.1	265.0	3.1
1373	286.5	295.3	3.1

[a] δ = (calc. − exp.)/exp. × 100

Table 2
Enthalpy increments of calcium niobate $Ca_2Nb_2O_7$

T (K)	$H_m(T) - H_m(298.15)$ (kJ mol^{-1}), experimental	$H_m(T) - H_m(298.15)$ (kJ mol^{-1}), integration of Eq. (5)	δ (%)[a]
774	125.9	122.4	−2.7
774	124.6	122.4	−1.7
874	147.1	150.5	2.3
874	151.1	150.6	−0.4
974	176.7	179.1	1.4
974	176.8	179.1	1.4
1074	204.9	208.1	1.6
1074	204.9	208.1	1.6
1174	233.3	237.6	1.8
1174	233.4	237.6	1.8
1274	262.1	267.4	2.0
1274	262.1	267.4	2.0
1373	297.0	297.4	0.1

[a] δ = (calc. − exp.)/exp. × 100

Debye temperature, as in this temperature range only the acoustic phonons are populated.

In the second step of the fit, both sets of the C_p data (relaxation time + DSC) were considered. All the estimated values were included into the simplex routine [20] and the full non-linear fit was performed on all adjustable parameters. Analysis of the phonon heat capacity was performed as an additive combination of Debye and Einstein models. The phonon spectrum of a polyatomic compound contains three acoustic branches and $3n-3$ optical ones, where n is number of atoms per formula unit. In our case, i.e. 11 atoms/f.u., this represents 30 optical branches. This approach is indeed a simplification, since n should properly refer to the number of atoms per primitive unit cell containing, in this instance, two formula units for S2N and four formula units for C2N. However, this would lead to an inadequate increase of parameters to be fitted. Both models include corrections for anharmonicity, which is responsible for a small, but not negligible, additive term at higher temperatures and which accounts for the discrepancy between isobaric and isochoric heat capacity. According to literature [21], the term $1/(1-\alpha T)$ is considered as a correction factor.

The acoustic part of the phonon heat capacity is then described using the Debye model in the form:

$$C_{\mathrm{phD}} = \frac{9R}{1-\alpha_{\mathrm{D}}T}\left(\frac{T}{\Theta_{\mathrm{D}}}\right)^3 \int_0^{x_{\mathrm{D}}} \frac{x^4 \exp(x)}{(\exp(x)-1)^2}\,\mathrm{d}x, \tag{1}$$

where R is the gas constant, Θ_{D} is the Debye characteristic temperature, α_{D} is the coefficient of anharmonicity of acoustic branches and $x_{\mathrm{D}} = \Theta_{\mathrm{D}}/T$. Here the three acoustic branches are taken as one triply degenerate branch. Similarly, the individual optical branches are described by the Einstein model:

$$C_{\mathrm{phEi}} = \frac{R}{1-\alpha_{\mathrm{Ei}}T} \cdot x_{\mathrm{Ei}}^2 \frac{\exp x_{\mathrm{Ei}}}{(\exp x_{\mathrm{Ei}}-1)^2}, \tag{2}$$

where α_{Ei} and x_{Ei} have analogous meanings as in the previous case. The phonon heat capacity then reads

$$C_{\mathrm{ph}} = C_{\mathrm{phD}} + \sum_{i=1}^{3n-3} C_{\mathrm{phEi}}. \tag{3}$$

To reduce the number of adjustable parameters, several optical branches are again grouped into one degenerate multiple branch with the same Einstein characteristic temperature and anharmonicity coefficient. This describes the 30 optical branches in terms of four Einstein modes with the respective degeneracies 4–8–8–10. The analysis of the phonon heat capacity is summarized in Table 3.

The values $H_m(298.15) - H_m(0) = 37{,}977 \pm 266\,\mathrm{J\,mol^{-1}}$ and $H_m(298.15) - H_m(0) = 35{,}631 \pm 215\,\mathrm{J\,mol^{-1}}$ for S2N and C2N, respectively, were obtained from the low-temperature C_{pm} data by numerical integration of the C_{pm} from 0 to 298.15 K. Standard deviations (2σ) were calculated with the error propagation law.

For the assessment of C_{pm} function above room temperature, the heat capacity data from DSC and the enthalpy increment data from drop calorimetry were treated simultaneously. As our measurements on the S2N sample were performed out of the incommensurate phase transition region, the derived equation holds for non-transition heat capacity only leaving out the C_{pm} anomaly in the vicinity of T_{INC} which was observed by other authors [1–3]. As the heat effect due to this transition is small compared to the enthalpy increments and their uncertainties, no additional corrections were made. Different weights w_i were assigned to individual points calculated as $w_i = 1/\delta_i$ where δ_i is the absolute deviation of the i-th measurement estimated from overall accuracies of the measurements (1% for DSC and 3% for drop

Table 3
Parameters for the phonon heat capacity

Type	Degeneracy	S2N		C2N	
		Characteristic temperature (K)	Anharmonicity coefficient (10^{-4} K^{-1})	Characteristic temperature (K)	Anharmonicity coefficient (10^{-4} K^{-1})
Acoustic	3	154 ± 1	0.7 ± 0.1	218 ± 1	0.5 ± 0.1
Optical	4	157 ± 1	0.5 ± 0.1	177 ± 1	0.5 ± 0.1
	8	307 ± 1	0.3 ± 0.1	382 ± 3	0.7 ± 0.1
	8	432 ± 1	0.6 ± 0.1	448 ± 6	0.7 ± 0.1
	10	900 ± 1	0.1 ± 0.1	880 ± 4	0.5 ± 0.1

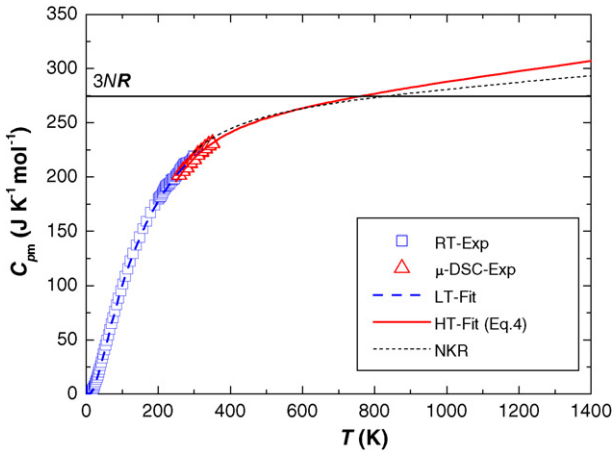

Fig. 3. Heat capacity of $Sr_2Nb_2O_7$.

calorimetry). Both types of experimental data thus gain comparable significance during the regression analysis. The temperature dependencies of the non-transition molar heat capacities of S2N and C2N (T = 298.15 – 1400 K) can thus be expressed by

$$\text{S2N}: C_{\text{pm}} = (248.0 \pm 3.9) + (0.04350 \pm 0.006301)T - \frac{(3.948 \pm 0.1998) \times 10^6}{T^2} (\text{J K}^{-1}\,\text{mol}^{-1}) \quad (4)$$

$$\text{C2N}: C_{\text{pm}} = (257.2 \pm 6.2) + (0.03621 \pm 0.01206)T - \frac{(4.435 \pm 0.2428) \times 10^6}{T^2} (\text{J K}^{-1}\,\text{mol}^{-1}). \quad (5)$$

The heat capacities as functions of temperature are shown in Figs. 3 and 4. The pertinent functions calculated according to the additivity Neumann–Kopp's rule (NKR) [22] are given for comparison. C_p data for CaO, SrO and Nb_2O_5 were taken from Refs. [23–25], respectively. While NKR predicts the heat capacities of S2N and C2N remarkably well from room temperature up to ~700 K, the differences between the two dependencies, $\Delta C_{p,ox}$, increase with increasing temperature. The prediction ability of NKR for mixed oxides was discussed in Refs. [26,27], but it seems impossible now to state in which cases NKR will estimate the heat capacity with acceptable uncertainty in the high-temperature region.

A comparison of our results with those of Akishige et al. [1] is given in Fig. 5. It follows that the agreement between these sets of data is very good in the temperature range 0–350 K. Then the broad C_p anomaly sets in with a maximum at 495 K which could not be detected by our measurements. However, a significant difference exists between our high-temperature fit and C_p data [1] above this transition temperature (≈15 J K^{-1} mol^{-1} at 600 K).

The values of standard molar entropies of S2N and C2N at 298.15 K S°_m(S2N, 298.15 K) = 238.5 ± 1.3 J K^{-1} mol^{-1} and S°_m(C2N, 298.15 K) = 212.4 ± 1.2 J K^{-1} mol^{-1} were derived from the low-temperature C_{pm} data by integrating the C_{pm}/T functions from 0 to 298.15 K. A numerical integration (trapezoidal rule) was used with the boundary conditions $S^\circ_m = 0$ and $C_{pm}/T = \gamma_{el}$ at T = 0 K. Standard deviations (2σ) were calculated using the error propagation law. Our value of entropy for S2N is in good agreement with S°_m(S2N, 298.15 K) = 232.37 J K^{-1} mol^{-1} derived from Akishige low-temperature C_{pm} data [1]. Using S°_m(SrO, 298.15 K) = 53.58 J K^{-1} mol^{-1} [24], S°_m(Nb_2O_5, 298.15 K) = 137.30 J K^{-1} mol^{-1} [25] and $\Delta_{f,ox}S$(S2N) = −39.93 J K^{-1} mol^{-1} [5] one can calculate S°_m(S2N, 298.15 K) = 204.53 J K^{-1} mol^{-1} which is obviously underestimated in comparison with third-law calorimetric data.

There are many other mixed oxides in the systems SrO–Nb_2O_5 and CaO–Nb_2O_5 and it should be useful to estimate still missing values of their entropies. Jenkins and Glasser [28,29] have

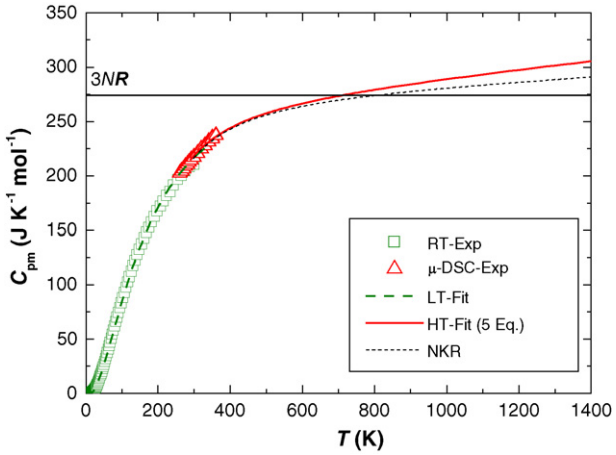

Fig. 4. Heat capacity of $Ca_2Nb_2O_7$.

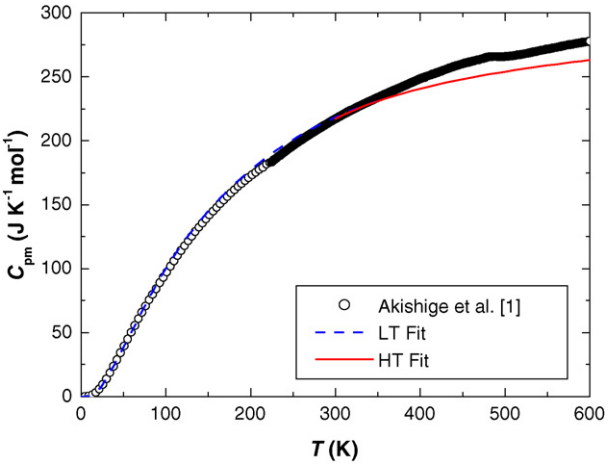

Fig. 5. Heat capacity of $Sr_2Nb_2O_7$; comparison of our results with those of Akishige et al. [1].

Table 4
Standard molar entropies at 298.15 K and formula unit volume of mixed oxides in the system Bi_2O_3–CaO–SrO–Nb_2O_5–Ta_2O_5

Oxide	V (nm^3 f.u.$^{-1}$)	$S_{m,exp.}$(298.15 K) (J K^{-1} mol^{-1})	$S_{m,calc.}$(298.15 K) (J K^{-1} mol^{-1})	δ (%)[a]
Bi_2O_3(monoclinic)	0.08173	148.5 [30]	130.3	−12.3
CaO(cubic)	0.02760	38.1 [23]	44.0	15.4
SrO(cubic)	0.03435	53.58 [24]	54.8	2.2
Nb_2O_5(monoclinic)	0.09778	137.30 [25]	155.9	13.5
Ta_2O_5(monoclinic)	0.08588	143.09 [25]	136.9	−4.3
$Bi_2Ca_2O_5$(triclinic)	0.14854	231.28 [7]	236.8	2.4
Bi_2CaO_4(monoclinic)	0.12128	188.46 [7]	193.3	2.6
$Bi_6Ca_4O_{13}$(orthorhombic)	0.37126	574.13 [7]	591.8	3.1
$BiNbO_4$(orthorhombic)	0.08270	147.86 [8]	131.8	−10.8
$BiTaO_4$(orthorhombic)	0.08212	149.11 [8]	130.9	−12.2
$SrBi_2Nb_2O_9$(orthorhombic)	0.19110	327.15 [10]	304.6	−6.9
$SrBi_2Ta_2O_9$(orthorhombic)	0.19087	339.23 [10]	304.2	−10.3
$SrNb_2O_6$(monoclinic)	0.11889	173.88 [11]	189.5	9.0
$Sr_2Nb_2O_7$(orthorhombic)	0.15111	232.37 [1]	240.9	3.7
$Sr_2Nb_2O_7$(orthorhombic)	0.15111	238.5[b]	240.9	1.0
$Sr_2Ta_2O_7$(orthorhombic)	0.15237	245.41 [1]	242.9	−1.0
$Ca_2Nb_2O_7$(monoclinic)	0.14021	212.4[b]	223.5	5.2
$CaNb_2O_6$(orthorhombic)	0.11170	167.40[c]	178.0	6.4

[a] δ = (calc. − exp.)/exp. × 100
[b] This work.
[c] Unpublished results.

proposed a linear correlation between the standard molar entropy at 298.15 K and the formula unit volume. This approach was used in the case of mixed oxides in the Bi_2O_3–CaO–SrO–Nb_2O_5–Ta_2O_5 system. The input data for correlation are summarized in Table 4. Only the third-law calorimetric values were considered here because high-temperature electromotive force measurements and the thermodynamic assessments in particular give less accurate data. Fig. 6 shows the results of the correlation. The linear relation is obvious and the straight line almost naturally passes through the origin: S_m(J K^{-1} mol^{-1}) = 1594V(nm^3 f.u.$^{-1}$), R^2 = 0.98. However, the mean relative error of estimated S_m values is about 7% which is too much in comparison with experimental errors of input calorimetric data. When only the mixed oxides (13 species) are considered, the correlation equation remains the same but the mean relative error of estimated S_m falls to 5.7%. It may be interesting to compare this approach with a simple additive scheme based on summing the entropies of constituent binary oxides ($\Delta_{f,ox}S$ = 0). For a set of mixed oxides given in Table 4 the mean relative error of calculated S_m values is 3.4%. For specific case of S2N and C2N under study, S_m is predicted, respectively, with an error 2.6% and 0.5% using the latter estimation.

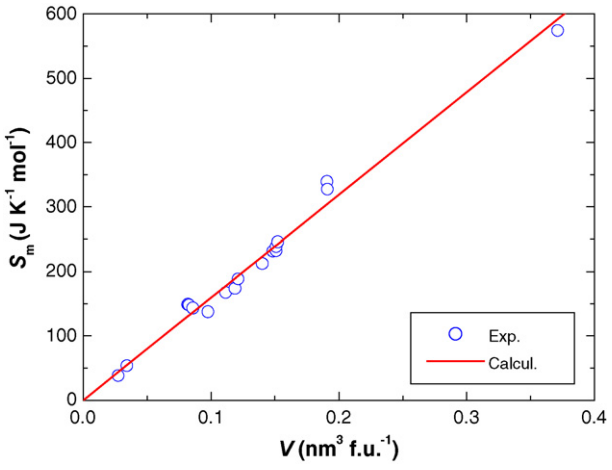

Fig. 6. Correlation between molar entropy and formula unit volume of selected mixed oxides in the system Bi_2O_3–CaO–SrO–Nb_2O_5–Ta_2O_5.

Acknowledgements

This work was supported by the Czech Science Foundation (grant No. 104/07/1209) and Ministry of Education of the Czech Republic (research projects No. MSM6046137302 and No. MSM6046137307). The work of P.S. is a part of the research program MSM0021620834 financed by the Ministry of Education of the Czech Republic.

Appendix A. Supplementary data

Supplementary data associated with this article can be found, in the online version, at doi:10.1016/j.tca.2008.06.010.

References

[1] Y. Akishige, H. Shigematsu, T. Tojo, H. Kawaji, T. Atake, J. Therm. Anal. Calorim. 81 (2005) 537;
Y. Akishige, H. Shigematsu, T. Tojo, H. Kawaji, T. Atake, Private communication, 2006.
[2] G. Shabbir, S. Kojima, J. Phys. D: Appl. Phys. 36 (2003) 1036.
[3] G. Shabbir, A. Hushur, J.-H. Ko, S. Kojima, J. Korean Phys. Soc. 42 (2003) S1294.
[4] Y. Yang, H. Yu, Z. Jin, J. Mater. Sci. Technol. 15 (1999) 203.
[5] J.R. Carruthers, M. Grasso, J. Electrochem. Soc. 117 (1970) 1426.
[6] S. Raghavan, J. Alloys Compd. 179 (1992) L25.
[7] P. Abrman, D. Sedmidubský, A. Strejc, P. Voňka, J. Leitner, Thermochim. Acta 381 (2002) 1.
[8] M. Hampl, A. Strejc, D. Sedmidubský, K. Růžička, J. Hejtmánek, J. Leitner, J. Solid State Chem. 179 (2006) 77.
[9] M. Hampl, J. Leitner, K. Růžička, M. Straka, P. Svoboda, J. Therm. Anal. Calorim. 87 (2007) 553.
[10] J. Leitner, M. Hampl, K. Růžička, D. Sedmidubský, P. Svoboda, J. Vejpravová, Thermochim. Acta 450 (2006) 105.
[11] J. Leitner, M. Hampl, K. Růžička, M. Straka, D. Sedmidubský, P. Svoboda, J. Therm. Anal. Calorim. 91 (2008) 985.
[12] J.S. Hwang, K.T. Lin, C. Tien, Rev. Sci. Instrum. 68 (1997) 94.
[13] W. Schnelle, J. Engelhardt, E. Gmelin, Cryogenics 39 (1999) 271.
[14] Quantum Design, Physical Property Measurement System – Application note, http://www.qdusa.com/pdf/brochures/heat.pdf.
[15] A.T. Dinsdale, CALPHAD 15 (1991) 317.
[16] J.W. Arblaster, Platinum Met. Rev. 38 (1994) 119.
[17] B. Wilthan, C. Cagran, C. Brunner, G. Pottlacher, Thermochim. Acta 415 (2004) 47.
[18] P. Daniels, R. Tamazyan, C.A. Kuntscher, M. Dressel, F. Lichtenberg, S. van Smaalen, Acta Crystallogr. B 58 (2002) 970.
[19] N. Ishizawa, F. Marumo, S. Iwai, M. Kimura, T. Kawamura, Acta Crystallogr. B 36 (1980) 763.
[20] W.H. Press, S.A. Teukolsky, W.T. Vetterling, B.P. Flannery, Numerical Recipes in FORTRAN, 2nd Edition, Cambridge University Press, 1992 (Chapter 10.4), pp. 402–406.

[21] C.A. Martin, J. Phys.: Condens. Matter 3 (1991) 5967.
[22] J. Leitner, P. Chuchvalec, D. Sedmidubský, A. Strejc, P. Abrman, Thermochim. Acta 395 (2003) 27.
[23] J.R. Taylor, A.T. Dinsdale, CALPHAD 14 (1990) 71.
[24] D. Risold, B. Hallstedt, L.J. Gauckler, CALPHAD 20 (1996) 353.
[25] O. Knacke, O. Kubaschewski, K. Hesselmann, Thermochemical Properties of Inorganic Substances, 2nd Edition, Springer, Berlin, 1991.
[26] P. Richet, G. Fiquet, J. Geophys. Res. 96 (1991) 445.
[27] L. Qiu, M.A. White, J. Chem. Educ. 78 (2001) 1076.
[28] H.D.B. Jenkins, L. Glaser, Inorg. Chem. 42 (2003) 8702.
[29] H.D.B. Jenkins, L. Glaser, Inorg. Chem. 45 (2006) 1754.
[30] D. Risold, B. Hallstedt, L.J. Gauckler, H.L. Lukas, S.G. Fries, J. Phase Equilib. 16 (1995) 223.